

# Temperature Dependence of Anisotropy Decay and Solvation Dynamics of Coumarin 153 in $\gamma$ -Cyclodextrin Aggregates

Durba Roy, Sudip Kumar Mondal, Kalyanasis Sahu, Subhadip Ghosh, Pratik Sen, and Kankan Bhattacharyya\*

Physical Chemistry Department, Indian Association for the Cultivation of Science, Jadavpur, Kolkata 700 032, India

Received: April 19, 2005; In Final Form: June 16, 2005

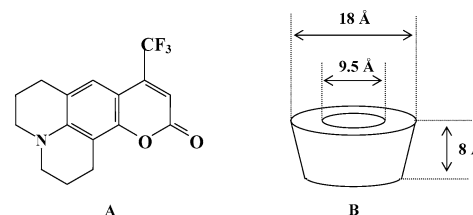
Effect of temperature on the fluorescence anisotropy decay and the ultraslow component of solvation dynamics of coumarin 153 (C153) in a  $\gamma$ -cyclodextrin ( $\gamma$ -CD) nanocavity are studied using a picosecond set up. The steady-state anisotropy ( $0.13 \pm 0.01$ ) and residual anisotropy ( $0.14 \pm 0.01$ ) in fluorescence anisotropy decay in an aqueous solution containing  $7 \mu\text{M}$  C153 and  $40 \text{ mM}$   $\gamma$ -CD are found to be quite large. This indicates formation of large linear nanotube aggregates of  $\gamma$ -CD linked by C153. It is estimated that  $>53$   $\gamma$ -CD units are present in each aggregate. In these aggregates with rise in temperature, the average solvation time ( $\langle\tau_s\rangle_{\text{obs}}$ ) decreases markedly from  $680 \text{ ps}$  at  $278 \text{ K}$  to  $160 \text{ ps}$  at  $318 \text{ K}$ . The dynamic Stokes shift is found to decrease from  $800 \text{ cm}^{-1}$  at  $278 \text{ K}$  to  $250 \text{ cm}^{-1}$  at  $318 \text{ K}$ . The fraction of dynamic Stokes shift ( $f_d$ ) detected in a picosecond set up is calculated using the Fee–Maroncelli procedure. The corrected solvation time ( $\langle\tau_s\rangle_{\text{corr}} = f_d\langle\tau_s\rangle_{\text{obs}}$ ) displays an Arrhenius type temperature dependence. From the temperature variation, the activation energy and entropy of the solvation process are determined to be  $12.5 \text{ kcal M}^{-1}$  and  $28 \text{ cal M}^{-1} \text{ K}^{-1}$ , respectively. The ultraslow component and its temperature dependence are ascribed to a dynamic exchange between bound and free water molecules.

## 1. Introduction

A cyclodextrin (CD) is a cyclic oligosaccharide consisting of six, seven, or eight glucose units respectively for  $\alpha$ ,  $\beta$ , and  $\gamma$ -CD.<sup>1,2</sup> They have a toroidal shape with a hydrophobic interior and two hydrophilic rims formed by the primary and secondary hydroxyl groups.<sup>1,2</sup> The height, inner and outer diameters of a  $\gamma$ -CD cavity are  $8$ – $9$ ,  $8$ , and  $18 \text{ \AA}$ , respectively (Scheme 1B).<sup>1</sup> In water (and several other polar solvents) a CD often encapsulates an organic molecule of suitable size to form a host–guest complex. Solubilization of an organic drug molecule in water using a CD cavity is extremely important in targeted drug delivery and has widespread application in pharmaceutical industry.<sup>2</sup> The ability to entrap an aromatic residue of a protein often imparts a chaperon-like property to a CD, and as such, cyclodextrin often prevents misfolding and aggregation of a protein to form fibrils.<sup>3</sup> Dynamics of a molecule confined in a nanocavity plays a key role in many biological processes. As a result, there have been many studies on organic fluorophores confined in a CD cavity.<sup>4–8</sup>

In a CD cavity, the rotational dynamics of the guest may be followed by fluorescence anisotropy decay using a fluorescent probe such as coumarin 153 (C153, Scheme 1A). According to the Stokes–Einstein formula, the time constant of anisotropy decay (rotational dynamics) increases with increase in the hydrodynamic size of the system (CD:guest). Balabai et al. earlier reported that anisotropy decay of a probe (oxazine) is slower inside CD cavity compared to that in bulk water and ascribed this to the larger size of the oxazine:CD complex compared to the oxazine molecule.<sup>5d</sup> Many groups have reported formation of large linear nanotube aggregates of cyclodextrins.<sup>6,7</sup>

SCHEME 1: (A) Coumarin 153 (C153) and (B)  $\gamma$ -Cyclodextrin



In these aggregates cyclodextrins are linked by linear surfactants<sup>6</sup> and also by aromatic guest molecules, e.g., diphenyl hexatriene (DPH)<sup>7a</sup> or diphenyl oxazole (PPO).<sup>7b,c</sup> In this work, using time-resolved anisotropy decay, we will show that similar large aggregates of  $\gamma$ -CD are formed in the presence of C153. We then report on solvation dynamics in this aggregate.

Fleming and co-workers first reported that in a cyclodextrin cavity ( $\gamma$ -CD), the solvation dynamics exhibits an ultraslow component on a  $1 \text{ ns}$  ( $1000 \text{ ps}$ ) time scale.<sup>8a</sup> This is substantially slower than the solvation dynamics in bulk water which exhibits a major component on a subpicosecond time scale with the longest component in  $\sim 1 \text{ ps}$ .<sup>9</sup> Subsequently, such a slow component on a  $100$ – $1000 \text{ ps}$  time scale has been detected in many other organized assemblies,<sup>8,10–17</sup> e.g., cyclodextrin in a nonaqueous solvent,<sup>8c</sup> protein,<sup>11</sup> micelle,<sup>12</sup> reverse micelle,<sup>13</sup> DNA,<sup>14</sup> nanoporous sol–gel glass,<sup>15</sup> lipid,<sup>16</sup> and polymer and polymer surfactant aggregates.<sup>17</sup>

Nandi and Bagchi<sup>19</sup> showed that the ultraslow component of solvation dynamics arises from a dynamic exchange between bound and free water.<sup>19</sup> The bound water molecules refers to the almost completely immobilized water molecules bound to a macromolecule (or cyclodextrin) by one or more hydrogen bonds and free water molecules are those which display bulk

\* Corresponding author. E-mail: pckb@mahendra.iacs.res.in. Fax: (91)-33-2473-2805.

water-like ultrafast dynamics. According to this model, the ultraslow component of solvation  $\tau_{\text{slow}} \approx k_{\text{bf}}^{-1}$ , where  $k_{\text{bf}}$  denotes the rate constant for bound-to-free interconversion. Assuming the transition state and “free” water molecules have similar free energy, energy, and entropy,  $k_{\text{bf}}$  is given by<sup>10,19</sup>

$$k_{\text{bf}} = \left( \frac{k_{\text{B}}T}{h} \right) \exp\left( \frac{-\Delta G_{\text{bf}}^0}{RT} \right) \quad (1)$$

where  $\Delta G_{\text{bf}}^0$  is the energy difference between free and bound water. Thus, this model predicts an Arrhenius type exponential decrease of solvation time with increase in temperature.

Recently, several groups reported on temperature dependence of solvation dynamics in ionic liquids<sup>18a</sup> and in micelles.<sup>18b</sup> Maroncelli and co-workers reported that in an ionic liquid average solvation time decreases about 10 times from 1.4 ns at 298 K to 0.15 ns at 355 K. We<sup>18b</sup> observed an 8-fold decrease in average solvation time in Triton X-100 (TX-100) micelle from 800 ps at 283 K to 100 ps at 323 K. From this, the activation energy of solvation dynamics is calculated to be  $\approx 9$  kcal mol<sup>-1</sup> in TX-100 micelle.<sup>18b</sup> According to eq 1, this corresponds to an energy difference of 8 kcal mol<sup>-1</sup> between bound and free water molecules. This is in remarkably good agreement with recent computer simulations.<sup>21a</sup>

According to computer simulation,<sup>21a</sup> the energy difference of a water–water and a water–micelle hydrogen bond, i.e., the energy difference between bound and free water, is 8 kcal mol<sup>-1</sup>. Most recently, several groups have carried out large scale computer simulations of solvation dynamics in proteins,<sup>20</sup> micelle,<sup>21</sup> reverse micelle,<sup>22</sup> and other confined systems and interfaces.<sup>23</sup> Many of these simulations reveal the presence of an ultraslow component (> 100 ps) of solvation dynamics.

In this work, we focus our attention on temperature dependence of solvation dynamics in a cyclodextrin aggregate.

## 2. Experimental Section

Coumarin 153 (C153, Scheme 1A) laser grade, Exciton, and  $\gamma$ -cyclodextrin ( $\gamma$ -CD, Fluka, Scheme 1B) were used as received. The steady-state absorption and emission spectra were recorded in a Shimadzu UV-2401 spectrophotometer and a Spex, FluoroMax-3 spectrofluorimeter, respectively. Viscosity of the 40 mM  $\gamma$ -CD solution was measured using a Ubbelohde viscometer. The solutions were prepared in double distilled with no buffer added.

For lifetime measurements, the samples were excited at 405 nm using a picosecond diode laser (IBH Nanoled-07) in an IBH Fluorocube apparatus. A Melles Griot filter (GG435) was used to block the exciting light and the emission was dispersed in a monochromator (IBH, model MCG-910 IB). The emission was collected at a magic angle polarization using a Hamamatsu MCP photomultiplier (5000U-09). The time correlated single photon counting (TCSPC) setup consists of an Ortec 9327 CFD and a Tennelec TC 863 TAC. The data are collected with a PCA3 card (Oxford) as a multichannel analyzer. The typical fwhm of the system response using a liquid scatterer is about 90 ps. The fluorescence decays were deconvoluted using IBH DAS6 software. The temperature was maintained using a bath circulator (Neslab, Endocal) with temperature accuracy of  $\pm 1$  °C.

To study fluorescence anisotropy decay, the analyzer was rotated at regular intervals to get perpendicular ( $I_{\perp}$ ) and parallel ( $I_{\parallel}$ ) components ( $\lambda_{\text{em}} = 490$  nm). Then the anisotropy function,

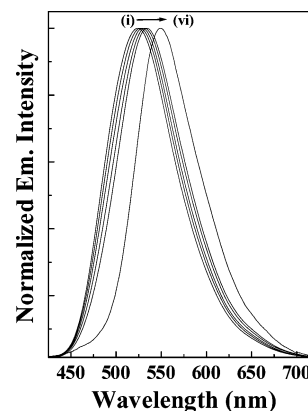


**Figure 1.** Normalized steady-state emission spectra of C153 ( $\lambda_{\text{ex}} = 405$  nm) in 40 mM  $\gamma$ -CD at (i) 278, (ii) 288, (iii) 296, (iv) 308, and (v) 318 K and (vi) in water (independent of temperature).

**TABLE 1: Parameters of Fluorescence Anisotropy Decay (Monitored at 490 nm) of 7  $\mu$ M C153 in 40 mM  $\gamma$ -Cyclodextrin at Different Temperatures**

temp (K)	$r(0)^a$	$r(\infty)^a$	$a_{R1}^a$	$\tau_{R1}^a$ (ps)	$a_{R2}^a$	$\tau_{R2}^a$ (ps)
278	0.26	0.14	0.22	100	0.78	1730
288	0.30	0.14	0.64	100	0.36	1350
296	0.26	0.14	0.31	100	0.69	1070
308	0.25	0.13	0.23	100	0.77	750
318	0.30	0.13	0.42	100	0.58	670

<sup>a</sup>  $\pm 10\%$ .

$r(t)$  was calculated using the formula

$$r(t) = \frac{I_{\parallel}(t) - GI_{\perp}(t)}{I_{\parallel}(t) + 2GI_{\perp}(t)} \quad (2)$$

The  $G$  value of the picosecond set up was determined using a probe whose rotational relaxation is very fast, e.g., coumarin 153 in methanol, and the  $G$  value was found to be 1.8.

## 3. Results and Discussion

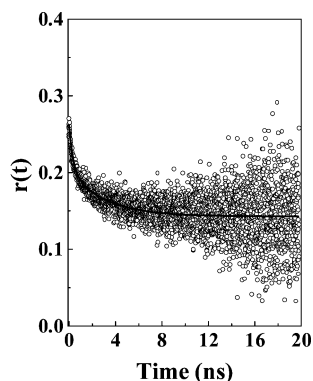
**3.1. Steady-State Emission Spectra.** In an aqueous solution, C153 exhibits emission maximum at 549 nm with emission quantum yield ( $\phi_f$ ) of 0.12.<sup>26</sup> Addition of  $\gamma$ -CD to a solution containing 7  $\mu$ M C153 results enhancement of emission intensity of C153 ( $\phi_f = 0.25$  at 40 mM  $\gamma$ -CD) with a gradual blue shift of the emission maximum to 530 nm in 40 mM  $\gamma$ -CD. The enhanced fluorescence and large blue shift in the emission maximum of C153 in  $\gamma$ -CD indicates that the probe experiences a lower polarity and more hydrophobic environment inside the  $\gamma$ -CD cavity than that in bulk water.<sup>5c</sup>

The emission spectrum of C153 in water does not show any temperature dependence. The emission spectrum of 7  $\mu$ M C153 in 40 mM  $\gamma$ -CD exhibits a temperature-dependent red shift from 524 nm at 296 K to 534 nm at 318 K with almost no change in the fluorescence intensity (Figure 1 and Table 2). The emission maximum of C153 displays a red shift with increase in solvent polarity.<sup>26</sup> From the temperature-dependent spectral shift it appears that the local polarity sensed by C153 inside the  $\gamma$ -CD cavity increases with the increase in temperature.

**3.2. Steady State and Time-Resolved Fluorescence Anisotropy Decay of C153 in  $\gamma$ -CD: Formation of Nanotube Aggregates.** The steady-state anisotropy of C153 in methanol or water was found to be  $0.015 \pm 0.005$ . This is close to the steady-state anisotropy value reported for other coumarin dyes.<sup>24</sup> In contrast to methanol or water, in 40 mM  $\gamma$ -CD the steady-state anisotropy of an aqueous solution containing 7  $\mu$ M C153

**TABLE 2: Steady State Emission Maxima, Observed  $\nu(0)$ , and Total Solvent Shift ( $\Delta\nu_{\text{obs}}$ ) for 7  $\mu\text{M}$  C153 in 40 mM  $\gamma$ -Cyclodextrin at Different Temperatures**

temp (K)	$\lambda_{\text{em}}^{\text{max}}$ (nm)	$\nu(0)^a$ ( $\text{cm}^{-1}$ )	$\Delta\nu_{\text{obs}}^a$ ( $\text{cm}^{-1}$ )
278	524	19 880	800
288	527	19 670	710
296	529	19 550	620
308	532	19 300	540
318	534	18 900	250

<sup>a</sup>  $\pm 100 \text{ cm}^{-1}$ .**Figure 2.** Fluorescence anisotropy decay of C153 ( $\lambda_{\text{ex}} = 405 \text{ nm}$  and  $\lambda_{\text{em}} = 490 \text{ nm}$ ) in 40 mM  $\gamma$ -CD at 278 K.

is found to be much higher ( $0.13 \pm 0.01$ ). The high steady-state anisotropy suggests that the microenvironment of C153 in 40 mM  $\gamma$ -CD is quite rigid. Similar high steady-state anisotropy is reported for DPH in  $\gamma$ -CD which is ascribed to formation of linear aggregates of  $\gamma$ -CD.<sup>7a</sup> To confirm formation of such aggregates, we studied time-resolved anisotropy decay of this system.

In bulk water, the time constant of fluorescence anisotropy decay of C153 (monitored at 490 nm) is  $100 \pm 20 \text{ ps}$  with no residual anisotropy decay. In the presence of 40 mM  $\gamma$ -CD, the fluorescence anisotropy decay of C153 (monitored at 490 nm) exhibits a large residual decay ( $0.14 \pm 0.01$ ) (Figure 2 and Table 1). The anisotropy decay of C153 in 40 mM  $\gamma$ -CD is fitted to a restricted rotor with residual anisotropy  $r(\infty)$  as

$$r(t) = r(\infty) + [r(0) - r(\infty)] \sum a_i \exp(-t/\tau_{R_i}) \quad (3)$$

The initial part of the anisotropy decay displays a fast component of  $100 \pm 20 \text{ ps}$  and a very slow component. The slow component of the anisotropy decay of C153 bound to  $\gamma$ -CD decreases from 1730 ps at 278 K to 670 ps at 318 K (Figure 2 and Table 1).

The residual anisotropy does not decay over 20 ns which is much larger than the lifetime of C153 ( $\sim 3.4 \text{ ns}$ ). This indicates that in 40 mM  $\gamma$ -CD the hydrodynamic size of the system is very large. According to Stokes–Einstein formula, the rotational time constant ( $\tau_R$ ) is related to viscosity ( $\eta$ ) and the volume

( $V$ ) of the C153:CD complex as<sup>5d,25</sup>

$$\tau_R = \frac{\eta V}{k_B T} \quad (4)$$

A 20 ns rotational time constant ( $\tau_R$ ) corresponds to a volume of  $V = 72\,800 \text{ \AA}^3$ . The linear aggregate of  $\gamma$ -CD is an ellipsoid with semiaxes  $a$ ,  $b$ , and  $c$  and volume  $V = 4\pi abc/3$ . In this case,  $a = b = 9 \text{ \AA}$  (same as that of  $\gamma$ -CD) while the length is  $2c$ . Thus, from the observed rotational time constant ( $\tau_R > 20 \text{ ns}$ ) the length of the aggregate,  $2c > 430 \text{ \AA}$ . This length is more than the height of 53  $\gamma$ -CD units (each of height  $8 \text{ \AA}$ ). Thus, the nanotube aggregate of C153 and  $\gamma$ -CD is a linear array containing more than 53  $\gamma$ -CD units. Previous workers also estimated that the linear aggregates joined by DPH and PPO contain  $>60$  cyclodextrin units.<sup>7</sup> Following Li and McGown,<sup>7a</sup> we propose the structure of the  $\gamma$ -CD aggregate linked by C153 as shown in Figure 3.

In summary, the large steady-state anisotropy and large residual anisotropy in the anisotropy decay indicate formation of linear aggregates of C153:CD. It may be noted that a part of the anisotropy decay remains fast. The fast initial components of anisotropy decay may be ascribed to wobbling and restricted rotation of the probe C153 (length  $10 \text{ \AA}$  and width  $8 \text{ \AA}$  according to MM2 calculation) inside the cavity of  $\gamma$ -CD (maximum inner diameter  $9.5 \text{ \AA}$ ) in the linear nanoaggregates.

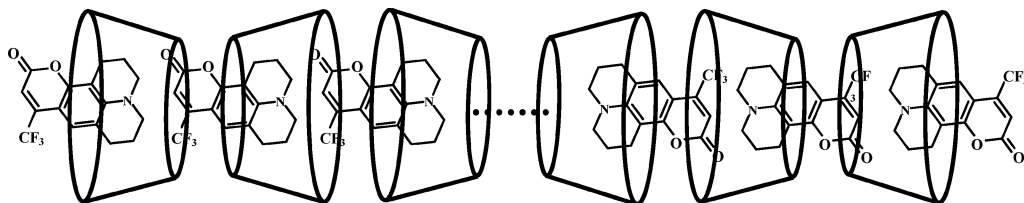
### 3.3. Time-Resolved Studies: Time Dependent Stokes Shift.

In this section, we discuss the temperature dependence of solvation dynamics of C153 in 40 mM  $\gamma$ -CD. At each temperature the fluorescence decays of 7  $\mu\text{M}$  C153 in 40 mM  $\gamma$ -CD strongly depends on the emission wavelengths. For example, at 278 K, the fluorescence decay of the blue end (455 nm) is found to be triexponential with decay components of 100 (62%), 750 (25%), and 3400 ps (13%). However, at the red end, 620 nm, the decay of time constants of 1270 and 4150 ps is preceded by a distinct rise of time constant of 360 ps as depicted in Figure 4. At 318 K, at the blue end (455 nm) the fluorescence decay of C153 in  $\gamma$ -CD is triexponential with decay components of 100 (48%), 790 (30%), and 3200 ps (22%). However, at the red end (620 nm) C153 exhibits a decay component of 860 and 3300 ps with a distinct growth component of 250 ps (Figure 5).

Time-resolved emission spectra (TRES) at different temperatures are constructed using the steady-state intensity and the fluorescence decay parameters following the method of Maroncelli and Fleming.<sup>27,28</sup> Figure 6 shows the TRES of C153 in 40 mM  $\gamma$ -CD at 278 K. The solvation dynamics is described by the decay of the solvent response function  $C(t)$ , defined by

$$C(t) = \frac{\nu(t) - \nu(\infty)}{\nu(0) - \nu(\infty)} \quad (5)$$

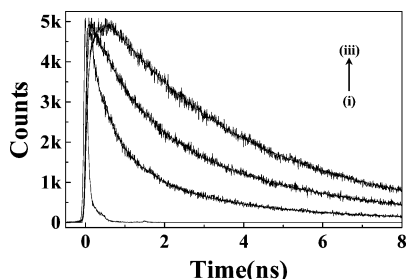
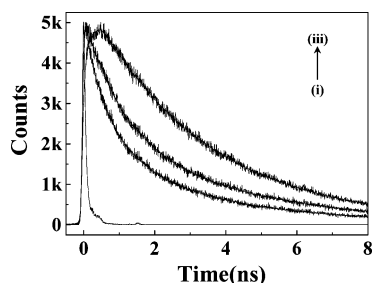
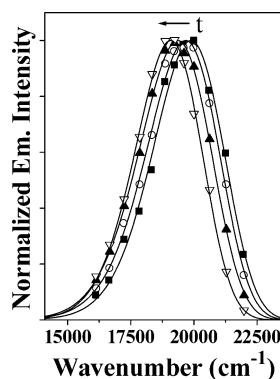
where  $\nu(0)$ ,  $\nu(t)$ , and  $\nu(\infty)$  are the emission frequencies at time zero,  $t$  and infinity. At 278 K, the solvation dynamics of C153 in 40 mM  $\gamma$ -CD is biexponential with a fast (170 ps) component

**Figure 3.** Model of C153:  $\gamma$ -CD linear aggregates.

**TABLE 3: Parameters Obtained from Decay of  $C(t)$  for C153 in 40 mM  $\gamma$ -Cyclodextrin at Different Temperatures**

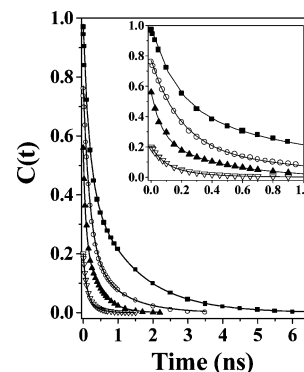
temp (K)	$\tau_1(a_1)^a$ (ps)	$\tau_2(a_2)^a$ (ps)	$\langle\tau_s\rangle_{\text{obs}}^{a,b}$ (ps)	fraction of total solvent shift detected ( $f_d$ )	$\langle\tau_s\rangle_{\text{corr}}^c$ (ps)
278	170 (55%)	1300 (45%)	680	0.97	660
288	190 (70%)	900 (30%)	400	0.76	300
296	100 (75%)	830 (25%)	280	0.64	180
308	60 (65%)	440 (35%)	190	0.56	110
318	90 (60%)	270 (40%)	160	0.20	30

<sup>a</sup>  $\pm 10\%$ . <sup>b</sup>  $\langle\tau_s\rangle_{\text{obs}} = a_1\tau_1 + a_2\tau_2$ . <sup>c</sup>  $\langle\tau_s\rangle_{\text{corr}} = f_d\langle\tau_s\rangle_{\text{obs}}$ .

**Figure 4.** Fluorescence decays of C153 in 40 mM  $\gamma$ -CD in water at 278 K at (i) 455, (ii) 485, and (iii) 600 nm.**Figure 5.** Fluorescence decays of C153 in 40 mM  $\gamma$ -CD in water at 318 K at (i) 455, (ii) 470, and (iii) 600 nm.**Figure 6.** Time-resolved emission spectra of C153 bound to 40 mM  $\gamma$ -CD in water at 0 (■), 100 (○), 500 (▲), and 6500 ps (▽) at 278 K.

(55%) and a slow component of 1300 ps (45%). The observed average solvation time ( $\langle\tau_s\rangle_{\text{obs}}$ ) is 680 ps (Figure 7, Table 3). However, at 318 K the decay of  $C(t)$  is characterized by two components of 90 (60%) and 270 ps (40%) with an average solvation time of 160 ps (Figure 7, Table 3). From Tables 2 and 3, it is obvious that as temperature increases solvation dynamics becomes faster, e.g. 680 ps at 278 K to 160 ps at 318 K. The observed dynamic Stokes shift also decreases from 800  $\text{cm}^{-1}$  (278 K) to 250  $\text{cm}^{-1}$  (318 K) (Table 2).

Because of the limited time resolution of a picosecond set up (90 ps in our case), a significant portion of the dynamic Stokes shift is missed. According to Fee and Maroncelli,<sup>28a</sup> the true emission frequency at time zero,  $\nu_{\text{em}}^{\text{p}}(0)$  may be calculated using the absorption frequency ( $\nu_{\text{abs}}^{\text{p}}$ ) of the system (23365  $\text{cm}^{-1}$

**Figure 7.** Decay of solvent response function,  $C(t)$  of C153 in 40 mM  $\gamma$ -CD in water at 278 (■), 288 (○), 308 (▲), and 318 K (▽). The points denote the actual values of  $C(t)$  and the solid line denotes the best fit to an exponential decay. Initial parts of the decays of  $C(t)$  are shown in the inset.

for C153 in 40 mM  $\gamma$ -CD),

$$\nu_{\text{em}}^{\text{p}}(0) = \nu_{\text{abs}}^{\text{p}} - [\nu_{\text{abs}}^{\text{np}} - \nu_{\text{em}}^{\text{np}}] \quad (6)$$

where  $\nu_{\text{em}}^{\text{np}}$  and  $\nu_{\text{abs}}^{\text{np}}$  respectively, denote the steady-state frequencies of emission and absorption of the probe in a nonpolar solvent. From eq 6 and using cyclohexane as a nonpolar solvent (absorption and emission maxima of C153 in cyclohexane are at 393<sup>26</sup> and 455 nm,<sup>26</sup> respectively) we have calculated the fraction ( $f_d$ ) of the total dynamic Stokes shift detected in our set up at each temperature (Table 3). It is observed that the fraction of the detected component also decreases from 0.97 (278 K) to 0.20 (318 K).

Since the contribution of the subpicosecond component of solvation dynamics to the average solvation times is very small, the corrected solvation time is given by

$$\langle\tau_s\rangle_{\text{corr}} \approx f_d\langle\tau_s\rangle_{\text{obs}} \quad (7)$$

The corrected average solvation time decreases drastically (about 20 times) from 660 (278 K) to 30 ps (318 K) (Table 3).

We now consider the possible origin of the ultraslow component of solvation dynamics. One possible source of the observed slow component could be the entry and exit of the probe from the cyclodextrin cavity. According to a recent experimental study,<sup>29a</sup> the entry and exit of an aromatic molecule from a CD cavity takes place in 100 ns time scale while a computer simulation<sup>29b</sup> indicates that a probe undergoes a piston like in and out motion in  $\sim 20$  ps time scale (five jumps in 100 ps). This is either too slow or too fast to explain the observed long component (100–1000 ps) of the solvent response.

In a recent work, it has been proposed that slow solvation dynamics of a probe in the water pool of a microemulsion involves self-diffusion of the probe from a less polar to a more polar region.<sup>13a</sup> The self-diffusion of the probe is manifested in the time dependent change in spectral width. However, in the present work at all temperatures, no such time dependent change



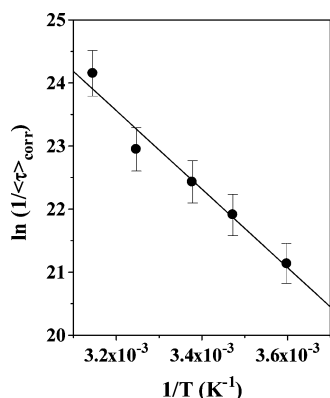


**Figure 8.** Plot of  $\ln(1/\langle\tau_s\rangle_{\text{corr}})$  against  $1/T$ .

in the emission spectral width is observed. This suggests self-motion of the probe C153 out of the CD cavity plays a minor role in the observed slow solvation dynamics.

Following Nandi and Bagchi<sup>19</sup> we ascribe the slow component of solvation dynamics to a dynamic exchange of free and bound (to cyclodextrin) water molecules. Equation 1 may be rewritten as

$$k_{\text{bf}} = \left(\frac{k_{\text{B}}T}{h}\right) \exp\left(\frac{\Delta S_{\text{bf}}}{R}\right) \exp\left(-\frac{E_{\text{a}}}{RT}\right) \quad (8)$$

Figure 8 shows a plot of  $\ln(1/\langle\tau_s\rangle_{\text{corr}})$  against  $1/T$  for  $7 \mu\text{M}$  C153 in  $40 \text{ mM}$   $\gamma$ -CD. The excellent linearity of the plot agrees with eqs 1 and 8. From the slope of Figure 8, the value of activation energy ( $E_{\text{a}}$ ) is calculated to be  $12.5 \text{ kcal M}^{-1}$ . Thus, the energy difference between water molecules in bulk and bound to cyclodextrin is estimated to be  $12.5 \text{ kcal M}^{-1}$ . From the intercept of the plot in Figure 8 and using eq 8 of entropy of activation ( $\Delta S$ ) for the slow solvation process of water molecules is found to be  $28 \text{ cal M}^{-1} \text{ K}^{-1}$ . According to Nandi–Bagchi model, the latter is approximately equal to the entropy difference of free and bound water molecules.

#### 4. Conclusion

From the time-resolved anisotropy decay, it is inferred that in an aqueous solution  $\gamma$ -CD nanotube aggregates are joined by C153. This work shows that in this nanoaggregate solvation dynamics of C153 in  $\gamma$ -CD exhibits marked temperature dependence. The activation energy of the solvation process is found to be  $12.5 \text{ kcal mol}^{-1}$ . The entropy of the solvation process is determined to be  $28 \text{ cal M}^{-1} \text{ K}^{-1}$ . The ultraslow component and the temperature dependence of solvation dynamics is attributed to a dynamic exchange between free and bound water molecules.

**Acknowledgment.** Thanks are due to Department of Science and Technology, India (Project Number: IR/11/CF-01/2002) and Council of Scientific and Industrial Research (CSIR) for generous research grants. D.R., S.K.M., K.S., and S.G. thank the CSIR for awarding fellowships. We also thank an anonymous reviewer for a helpful suggestion.

#### References and Notes

- (1) (a) Saenger, W. In *Inclusion Compounds*; Atwood, J. L., Davies, J. E., MacNicol, D. D., Eds. Academic: New York, 1984, Vol. 2, p 231. (b) Bender, M. L.; Komiyama, M. *Cyclodextrin Chemistry*; Springer-Verlag: New York, 1978, Chapter 3. (c) Szteli, J. *Chem. Rev.* **1998**, *98*, 1743. (d) Li, S.; Purdy, W. C. *Chem. Rev.* **1992**, *92*, 1457.
- (2) Uekama, K.; Hirayama, F.; Irie, T. *Chem. Rev.* **1998**, *98*, 2045.

- (3) Khajehpour, M.; Troxler, T.; Nanda, V.; Vanderkooi, J. M. *Proteins* **2004**, *55*, 275.
- (4) (a) Douhal, A. *Chem. Rev.* **2004**, *104*, 1955. (b) Bortulus, P.; Monti, S. *Adv. Photochem.* **1995**, *21*, 1. (c) Bhattacharyya, K.; Chowdhury, M. *Chem. Rev.* **1993**, *93*, 507.
- (5) (a) Scypinski, S.; Drake, J. M. *J. Phys. Chem.* **1985**, *89*, 2432. (b) Nag, A.; Chakraborty, T.; Bhattacharyya, K. *J. Phys. Chem.* **1990**, *94*, 4203. (c) Bergmark, W. R.; Davis, A.; York, C.; Macintosh, A.; Jones, G., II. *J. Phys. Chem.* **1990**, *94*, 5020. (d) Balabai, N.; Linton, B.; Nappaer, A.; Priyadarshi, S.; Sukharevsky, A. P.; Waldeck, D. H. *J. Phys. Chem. B* **1998**, *102*, 9617. (e) Hansen, J. E.; Pines, E.; Fleming, G. R. *J. Phys. Chem.* **1992**, *96*, 6904.
- (6) (a) Okada, M.; Harada, A. *Org. Lett.* **2004**, *6*, 361. (b) Harada, A. *Acc. Chem. Res.* **2001**, *34*, 456. (c) Nepogodiev, S. A.; Stoddart, J. F. *Chem. Rev.* **1998**, *98*, 1959.
- (7) (a) Li, G.; McGown, L. B. *Science* **1996**, *264*, 249. (b) Agbaria, R. A.; Gill, D. *J. Phys. Chem.* **1988**, *92*, 1052. (c) Agnew, K. A.; McCauley, T. D.; Agbaria, R. A.; Warner, I. M. *J. Photochem. Photobiol. A* **1995**, *91*, 205.
- (8) (a) Vajda, S.; Jimenez, R.; Rosenthal, S. J.; Fidler, V.; Fleming, G. R.; Castner, E. W., Jr. *J. Chem. Soc. Faraday Trans.* **1995**, *91*, 867. (b) Nandi, N.; Bagchi, B. *J. Phys. Chem.* **1996**, *100*, 13914. (c) Sen, S.; Sukul, D.; Dutta, P.; Bhattacharyya, K. *J. Phys. Chem. A* **2001**, *105*, 10635.
- (9) (a) Jimenez, R.; Fleming, G. R.; Kumar, P. V.; Maroncelli, M. *Nature (London)* **1994**, *369*, 471. (b) Fecko, C. J.; Eaves, J. D.; Loparo, J. J.; Tokmakoff, A.; Geissler, P. L. *Science* **2003**, *301*, 1698. (c) Jarzaba, W.; Walker, G. C.; Johnson, A. E.; Kahlow, M. A.; Barbara, P. F. *J. Phys. Chem.* **1988**, *92*, 7039. (d) Nandi, N.; Roy, S.; Bagchi, B. *J. Chem. Phys.* **1995**, *102*, 1390.
- (10) (a) Nandi, N.; Bhattacharyya, K.; Bagchi, B. *Chem. Rev.* **2000**, *100*, 2013. (b) Bhattacharyya, K.; Bagchi, B. *J. Phys. Chem. A* **2000**, *104*, 10603. (c) Bhattacharyya, K. *Acc. Chem. Res.* **2003**, *36*, 95. (d) Pal, S. K.; Zewail, A. H. *Chem. Rev.* **2004**, *104*, 2099.
- (11) (a) Jordanides, X. J.; Lang, M. J.; Song, X.; Fleming, G. R. *J. Phys. Chem. B* **1999**, *103*, 7995. (b) Pal, S. K.; Mandal, D.; Sukul, D.; Sen, S.; Bhattacharyya, K. *J. Phys. Chem. B* **2001**, *105*, 1438.
- (12) (a) Hara, K.; Kuwabara, H.; Kajimoto, O. *J. Phys. Chem. A* **2001**, *105*, 7174. (b) Mandal, D.; Sen, S.; Tahara, T.; Bhattacharyya, K. *Chem. Phys. Lett.* **2002**, *359*, 77. (c) Shirota, H.; Tamoto, Y.; Segawa, H. *J. Phys. Chem. A* **2004**, *108*, 3244.
- (13) (a) Dutta, P.; Sen, P.; Mukherjee, S.; Halder, A.; Bhattacharyya, K. *J. Phys. Chem. B* **2003**, *107*, 10815. (b) Satoh, T.; Okuno, H.; Tominaga, K.; Bhattacharyya, K. *Chem. Lett.* **2004**, *33*, 1090. (c) Willard, D. M.; Riter, R. E.; Levinger, N. E. *J. Am. Chem. Soc.* **1998**, *120*, 4151. (d) Corbeil, E. M.; Riter, R. E.; Levinger, N. E. *J. Phys. Chem. B* **2004**, *108*, 10777.
- (14) (a) Gearheart, L. A.; Somoza, M. M.; Rivers, W. E.; Murphy, C. J.; Coleman, R. S.; Berg, M. A. *J. Am. Chem. Soc.* **2003**, *125*, 11812. (b) Brauns, E. B.; Madaras, M. L.; Coleman, R. S.; Murphy, C. J.; Berg, M. A. *Phys. Rev. Lett.* **2002**, *88*, 158101–1.
- (15) (a) Scodinu, A.; Reilly, T.; Fourkas, J. T. *J. Phys. Chem. B* **2002**, *106*, 1041. (b) Farrer, R. A.; Fourkas, J. T. *Acc. Chem. Res.* **2003**, *36*, 605. (c) Sen, P.; Mukherjee, S.; Patra, A.; Bhattacharyya, K. *J. Phys. Chem. B* **2005**, *109*, 3319. (d) Baumann, R.; Ferrante, C.; Kneuper, E.; Deeg, F.-W.; Brauchle, C. *J. Phys. Chem. A* **2003**, *107*, 2422.
- (16) (a) Pal, S. K.; Sukul, D.; Mandal, D.; Bhattacharyya, K. *J. Phys. Chem. B* **2000**, *104*, 4529. (b) Sykora, J.; Kapusta, P.; Fidler, V.; Hof, M. *Langmuir* **2002**, *18*, 571. (c) Chattopadhyay, A.; Mukherjee, S. *Langmuir* **1999**, *15*, 2142.
- (17) (a) Frauchiger, L.; Shirota, H.; Uhrich, K. E.; Castner, E. W., Jr. *J. Phys. Chem. B* **2002**, *106*, 7463. (b) Sen, S.; Sukul, D.; Dutta, P.; Bhattacharyya, K. *J. Phys. Chem. B* **2002**, *106*, 3763. (c) Halder, A.; Sen, P.; Das Burman, A.; Bhattacharyya, K. *Langmuir* **2004**, *20*, 653.
- (18) (a) Ingram, J. A.; Moog, R. S.; Ito, N.; Biswas, R.; Maroncelli, M. *J. Phys. Chem. B* **2003**, *107*, 5926. (b) Sen, P.; Mukherjee, S.; Halder, A.; Bhattacharyya, K. *Chem. Phys. Lett.* **2004**, *385*, 357.
- (19) Nandi, N.; Bagchi, B. *J. Phys. Chem. B* **1997**, *101*, 10954.
- (20) (a) Bandyopadhyay, S.; Chakraborty, S.; Balasubramanian, S.; Bagchi, B. *J. Am. Chem. Soc.* **2005**, *127*, 4071. (b) Marchi, M.; Sterpone, F.; Ceccarelli, M. *J. Am. Chem. Soc.* **2002**, *124*, 6787.
- (21) (a) Pal, S.; Balasubramanian, S.; Bagchi, B. *J. Phys. Chem. B* **2003**, *107*, 5194. (b) Balasubramanian, S.; Pal, S.; Bagchi, B. *Phys. Rev. Lett.* **2002**, *89*, 115505–1. (c) Bruce, C. D.; Senapati, S.; Berkowitz, M. L.; Perera, L.; Forbes, M. D. E. *J. Phys. Chem. B* **2002**, *106*, 10902.
- (22) (a) Faeder, J.; Ladanyi, B. M. *J. Phys. Chem. B* **2005**, *109*, 6732. (b) Senapati, S.; Chandra, S. *J. Phys. Chem. B* **2001**, *105*, 5106. (c) Senapati, S.; Berkowitz, M. L. *J. Chem. Phys.* **2003**, *118*, 1937.
- (23) (a) Thompson, W. H. *J. Chem. Phys.* **2002**, *117*, 6618. (b) Thompson, W. H. *J. Chem. Phys.* **2004**, *120*, 8125. (c) Gomez, J. A.; Thompson, W. H. *J. Phys. Chem. B* **2004**, *108*, 20144. (d) Michael, D.; Benjamin, I. *J. Chem. Phys.* **2001**, *114*, 2817.

- (24) Dutt, G. B.; Raman, S. *J. Chem. Phys.* **2001**, *114*, 6702.
- (25) (a) Quitevis, E. L.; Marcus, A. H.; Fayer, M. D. *J. Phys. Chem.* **1993**, *97*, 5762. (b) Wittouck, N. W.; Negri, R. M.; De Schryver, F. C. *J. Am. Chem. Soc.* **1994**, *116*, 10601. (c) Krishna, M. G. M.; Das, R.; Periasamy, N.; Nityananda, R. *J. Chem. Phys.* **2000**, *112*, 8502. (d) Dutta, G. B. *J. Phys. Chem. B* **2003**, *107*, 10546. (e) Sen, S.; Sukul, D.; Dutta, P.; Bhattacharyya, K. *J. Phys. Chem. A* **2001**, *105*, 7495.
- (26) Jones, G.; II; Jackson, W. R.; Choi, C.-Y.; Bergmark, W. R. *J. Phys. Chem.* **1985**, *89*, 294.
- (27) Maroncelli, M.; Fleming, G. R. *J. Chem. Phys.* **1987**, *86*, 6221.
- (28) (a) Fee, R. S.; Maroncelli, M. *Chem. Phys.* **1994**, *183*, 235. (b) Horng, M. L.; Gardecki, J. A.; Papazyan, A.; Maroncelli, M. *J. Phys. Chem.* **1995**, *99*, 17311.
- (29) (a) Okano, L. T.; Barros, T. C.; Chou, D. T. H.; Bennet, A. J.; Bohne, C. *J. Phys. Chem. B* **2001**, *105*, 2122. (b) van Helden, S. P.; van Eyck, B. P.; Mark, A.; van Gunsteren, W. F.; Janssen, L. H. M. In *The Sixth International Cyclodextrin Symposium, Chicago 1992, Abstract*, 1992; p L-24.